

Robust quantum state engineering through coherent localization in biased-coin quantum walks

H. Majury^{1,2}, J. Boutari³, E. O’Sullivan¹, A. Ferraro², and M. Paternostrò²

¹Centre for Secure Information Technologies (CSIT), Queens University, Belfast BT7 1NN, United Kingdom

²Centre for Theoretical Atomic, Molecular and Optical Physics,
School of Mathematics and Physics, Queen’s University, Belfast BT7 1NN, United Kingdom

³Clarendon Laboratory, University of Oxford, Parks Road, Oxford OX1 3PU, UK

(Dated: December 9, 2024)

We address the performance of a coin-biased quantum walk as a generator for non-classical position states of the walker. We exploit a phenomenon of *coherent localisation* in the position space — resulting from the choice of small values of the coin parameter and assisted by post-selection — to engineer large-size coherent superpositions of distinguishable position states of the walker. The protocol that we design appears to be remarkably robust against both the actual value taken by the coin parameter and strong dephasing-like noise acting on the spatial degree of freedom. We finally illustrate a possible linear-optics implementation of our proposal, suitable for both bulk and integrated-optics platforms.

Quantum walks, which generalize the well-known concept of random walks to the quantum domain, have recently attracted considerable attention in light of the possibility that they offer the capability to explore non-trivial phenomena in statistical mechanics [1], such as interference [2], localization [3] and tunnelling, and are able to establish entanglement among either the different degrees of freedom of a walker, or the parties of a multi-walker setting [4]. Quantum walk-based architectures for quantum computation have been proposed and theoretically explored [5], while the possibility to implement quantum simulation through schemes based on the dynamics of a quantum walker are currently being pursued both theoretically and experimentally.

In the last few years, the number of experimental validations of the quantum walk paradigm, and investigations towards its use for the coherent manipulation of information at the quantum mechanical level have flourished [6–9]. This therefore paves the way to the full exploitation of the possibilities offered by quantum walks for quantum state engineering in Hilbert spaces of large dimensions, which is in general a difficult task to pursue experimentally. In this paper, we explore exactly such a possibility and exploit the peculiar statistical features of a discrete-time quantum walk to engineer non-classical states of an N -dimensional system. Specifically, we make use of special *coherent localization effects* induced on the position state of a quantum walker by choosing properly the operation describing the tossing of a coin. We demonstrate that high-quality coherent superpositions of fully distinguishable position states of the walker can be arranged through this mechanism and simple post-processing operations. Moreover, we assess the robustness of our scheme against improper choices of the coin operation, showing that the scheme remains effective in a broad range of possible choices for such a transformation. Remarkably, such robustness extends to the effects of a dephasing environment that projects the state of the walker onto position states with no quantum coherence. Finally, we assess the experimental observability of the effects that we predict, showing that both bulk- and integrated-optics settings are suitable for such scope.

The remainder of this paper is organised as follows: Sec. I illustrates the basic features of the quantum walk at hand and present the effects induced by the use of a so-called Pauli

\hat{Z} operator. This will be sufficient to provide an intuition of the physical influences that low-parameter coin operations have on the statistical features of the walk. Sec. II discusses the effects that deviations from the ideal conditions stated in Sec. I have on the features of the walk, and how postselection aids in generating superposition states of the walker’s position. Sec. III discusses the case of a special preparation of the walker, and how this results in a quantum coherent superposition of spatial distributions, while Sec. IV illustrates a possible experimental implementation encompassing the features at the core of our analysis. Finally, Sec. V presents our conclusion.

I. QUANTUM WALK WITH SU(2) COIN OPERATION

The one-dimensional discrete-time quantum random walk (DTQRW) entails a ‘walker’ endowed with two distinct degrees of freedom: a spatial one, which we dub ‘position’, and an internal one, which embodies the ‘coin’ that is tossed to decide the direction of the movement of the walker. The position state refers to where the walker is, in relation to the centre of the line on which it is moving. In the case of a linear walk and a dichotomic coin, the basis of the Hilbert space for such degrees of freedom are $\mathcal{H}_p : \{|n\rangle_p; n \in \mathbb{Z}\}$ and $\mathcal{H}_c : \{|0\rangle_c, |1\rangle_c\}$, respectively.

Each step of the evolution comprises a coin-tossing operation and a position shift. The first can be formally described using the unitary coin transformation

$$\hat{C}_c(\theta) = \cos \theta \hat{Z}_c + \sin \theta \hat{X}_c \quad (1)$$

with $\hat{X}, \hat{Y}, \hat{Z}$ the x, y, z Pauli spin operator acting in \mathcal{H}_c . Although this is not the most general form of coin operation that can be devised, it captures the essence of the features that we aim at addressing in this work. Typically, the Hadamard coin $\hat{C}_c(\pi/4)$ is used, which yields equal probabilities for the walker to move leftward or rightward [12]. The shift operator acts on the position of the walker, conditionally on the state of

the coin as

$$\begin{aligned}\hat{S} &= \exp[i\hat{P}_p \otimes \hat{Z}_c] \\ &= \sum_n \left[|n+1\rangle \langle n|_p \otimes |0\rangle \langle 0|_c + |n-1\rangle \langle n|_p \otimes |1\rangle \langle 1|_c \right]\end{aligned}\quad (2)$$

with $\hat{S}|N, 0\rangle_{p,c} = \hat{S}|-N, 1\rangle_{p,c} = 0$ for a $2N + 1$ -site position space (for as walk on a linear lattice) centred in $n = 0$. In what follows, we will study the effect of specific non-unitary maps on the dynamics of the walk. Therefore, we adopt a description based on density matrices right from this point, where $\hat{\rho}_{pc}(t)$ is the joint state of walker and coin at the discrete time t of their evolution. With the notation introduced above we have

$$\hat{\rho}_{pc}(t) = [\hat{S} \hat{C}_c(\theta)] \hat{\rho}_{pc}(t-1) [\hat{S} \hat{C}_c(\theta)]^\dagger. \quad (3)$$

Unless otherwise specified, it is intended that at the end of the walk the coin is traced out to leave room for an analysis of the statistical properties of the spatial degree of freedom. In this context, a key quantity in the study of quantum walk dynamics is the probability $P(n) = {}_p \langle n | \text{Tr}_c[\hat{\rho}_{pc}(t)] | n \rangle_p$ that position n in the position space is occupied at the discrete time t .

The one-dimensional DTQRW with a Hadamard coin (dubbed here a Hadamard walk) has been the focus of extensive research activities both at the theoretical and experimental level [1, 10]. The most striking feature of a Hadamard walk is the quadratic growth of the variance of the walk with the size of the lattice, a property that makes the DTQRW very useful for the design of faster-than-classical search algorithms.

On the contrary, walks with $\theta \neq \pi/4$ (thus resulting in unequal chances for the walker to move leftward and rightward) have received only limited attention [12]. Yet, interesting features emerge from considering biased coin operations. Most noticeably, for an N -step DTQRW achieved using $\hat{C}_c(\theta)$, the variance of the walk has been shown to vary as [12]

$$\sigma_\theta^2 \sim (1 - \sin \theta) N^2, \quad (4)$$

which, for $\theta \in [0, \pi/4)$, is larger than that of a Hadamard walk. Notice that the initial state considered in Ref. [12] is the factorized pure state

$$\hat{\rho}_{pc}(0) = |0\rangle \langle 0|_p \otimes |\phi\rangle \langle \phi|_c, \quad (5)$$

with $|\phi\rangle_c = \frac{1}{\sqrt{2}}(|0\rangle + i|1\rangle)_c$.

Our goal is to further explore the features of a low- θ walk to see what properties of the walk are dependant on this choice of coin operation, and the extent of the control that can be operated on the walk through the tuning of such operation. The behaviour for low- θ described by Eq. (4) can be intuitively understood considering the limit case of $\theta = 0$, corresponding to a Pauli \hat{Z}_c coin operation. For a generic initial pure state of the walker $|\psi_0\rangle_p$, the state of the system after t steps reads

$$|\Psi(t)\rangle_{pc} = \frac{1}{\sqrt{2}} \left[|\psi_{-t}\rangle_p |0\rangle_c + i(-1)^t |\psi_{+t}\rangle_p |1\rangle_c \right], \quad (6)$$

where the walker states $|\psi_{\pm t}\rangle_p$ are defined as the initial state $|\psi_0\rangle_p$ displaced by $\pm t$ steps in the position space \mathcal{H}_p

$$|\psi_{\pm t}\rangle_p = \sum_n |n \pm t\rangle_p \langle n | \psi_0 \rangle_p. \quad (7)$$

Eq. (6) shows that, regardless of the initial state of the walker, the dynamics generates a maximally entangled state between the coin and walker, in which the state of the latter is rigidly displaced towards the extremes of \mathcal{H}_p . Therefore, if the initial state $|\psi_0\rangle_p$ is localised in the position state, we have a coherent superposition of two states localized towards the opposite ends of the walker line. In addition, the absence of quantum interference in the position space explains the larger variance of the \hat{Z}_c -walk with respect to the Hadamard walk, as per Eq. (4).

II. DEVIATIONS FROM AN IDEAL \hat{Z}_p -WALK

Given the behaviour just described, a natural question arises: are the main features of the \hat{Z}_c -walk — namely, the generation of maximal entanglement and large variance — robust against imperfections? Here we will focus on two main sources of imperfections. First, we will consider the case in which the coin parameter θ is different from zero. Second, we will take into account the detrimental effect of noise on the walk.

A. Robustness to small θ deviations

We first look at the ideal scenario corresponding to the full absence of noise and arbitrary θ , in order to gain insight into the phenomenology of the walk. Considering the initial state in Eq (5), Fig. 1 shows the probability distribution $P(n)$ of finding the walker at the n^{th} site of a lattice after $N = 100$ steps when the coin parameter is increased.

The effects of such variations on the probability distribution of the walk are significant: As θ increases from $\pi/4$, the spread of the walk decreases, while a decrease of θ from the value corresponding to a Hadamard walk results in the walker being able to spread faster and visit more sites of the lattice, in line with Ref. [12]. Remarkably, for small values of the coin parameter, the walker manages to spread to all the sites on the line, reaching the end-site on the position space [cf. Fig. 1 (d)]. Similarly to what is observed for the ideal \hat{Z}_c -walk, there is a strong modification of the interference mechanism responsible for the features of a quantum walk. This results in a significant reduction of the probability for the walker to occupy sites on the lattice that are different from those close to the end of the position space. A closer look reveals that a small value of the coin parameter effectively localizes the walker around $n = \pm N$ in a coherent way (the underlying dynamics of the walker is fully unitary, at this stage), although the probability for the walker to occupy *exactly* such end sites appears to depend on the size of the position space itself: smaller spaces result in larger fidelity at a given value of θ . This is shown

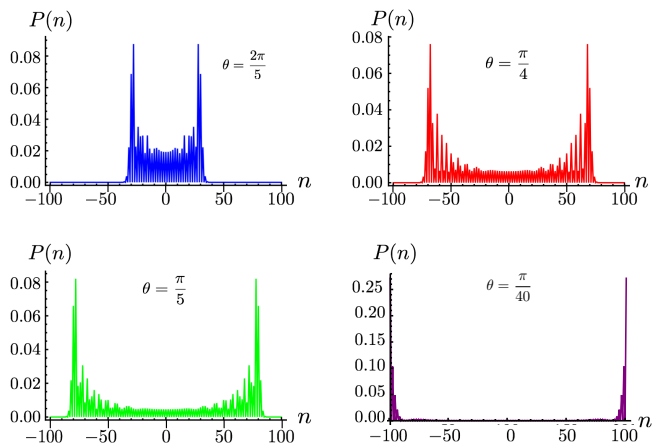


FIG. 1. (Color online) **(a)** Probability distributions for the DTQRW with initial state $|0\rangle_p \otimes |\phi\rangle_c$ [with $|\phi\rangle_c$ as in Eq. (5)] for varying coin parameter θ and $N = 100$ steps. As θ decreases, the walk spreads much wider on the lattice, thus enabling the walker to visit more sites on the line. For $\theta = \pi/40$ the walker manages to spread to all the sites on the line, reaching the end-site at the end-lattice positions $|-100\rangle_p$ and $|100\rangle_p$. Moreover, the probability to occupy sites different from the end ones is strongly reduced, thus manifesting a pronounced coherent localisation effect of the walker.

in Fig. 2 **(a)**, where we plot the state fidelity [13] between the final position state of the walker for a $2N + 1$ -dimensional position space and coherent superposition states of the form $(|-N + k\rangle_p \pm |N - k\rangle_p)/\sqrt{2}$ (for $k = 0, 1, 2, \dots$) against the value taken by the coin parameter and for growing sizes of the position space (we plot the largest of the two fidelities). While the fidelity with the state with $k = 0$ decreases as the coin parameter grows, the state of the position degree of freedom becomes close to coherent superposition states with growing values of k , as witnessed by the *ripples* displayed in Fig. 2 **(a)**.

Notice that, in the case of a \hat{Z}_c -walk, the walker-coin entanglement and the rigid translation of the initial state towards

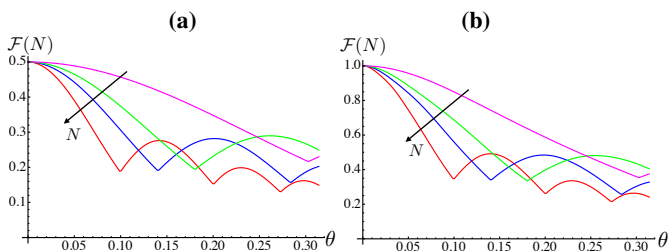


FIG. 2. (Color online) **(a)** Fidelity between the coherent superposition state $(|-N + k\rangle_p \pm |N - k\rangle_p)/\sqrt{2}$ (with $k = 0, 1, 2, 3$) and the position state of the walker after $N = 10$ (magenta), $N = 30$ (green), $N = 50$ (blue) and $N = 100$ (red curve) steps, plotted against the coin parameter θ . The initial monotonically decreasing trait of each curve corresponds to the fidelity with the state with $k = 0$. The first *ripple* is for $k = 1$, and so on. **(b)** Same as panel **(a)** but for the conditional state of the walker achieved by projecting the coin onto its initial state.

the extremes of the walker line implies a final walker state $\hat{\rho}_p(N) = \frac{1}{2}(|N\rangle\langle N| + |-N\rangle\langle -N|)$. The latter has a fidelity $\mathcal{F} = 1/2$ for $k = 0$ independently of N which explains the low fidelity of Fig. 2 **(a)**. We can see that, in case of low θ , the residual entanglement established between coin and position of the walker prevents the state of the walker from exhibiting strong coherences between $|N - k\rangle$ and $|-N + k\rangle$. The absence of such coherences is the factor limiting the values taken by the fidelity studied in Fig. 2 **(a)**. The situation can be significantly modified if we slightly change our approach to the determination of the position state of the walker: rather than tracing out the coin after the N -step walk, we projectively measure the coin state in the basis determined by $\{|\phi\rangle_c, |\phi_\perp\rangle_c \equiv \frac{1}{\sqrt{2}}(i|0\rangle + |1\rangle)_c\}$. That is, we consider the conditional position state

$$\hat{\rho}_p^j(N) = \frac{\hat{\Pi}_c^j \hat{\rho}_{pc}(N) \hat{\Pi}_c^j}{\text{Tr}[\hat{\Pi}_c^j \hat{\rho}_{pc}(N)]}, \quad (8)$$

where $j = 0, 1$ and $\hat{\Pi}_c^0 \equiv |\phi\rangle\langle\phi|_c$ and $\hat{\Pi}_c^1 \equiv |\phi_\perp\rangle\langle\phi_\perp|_c$. Notice that in the case of a \hat{Z}_c -walk, one has

$$\hat{\rho}_p^j(N) = \tau_p^j(N) \equiv \frac{1}{2} \left[|-N\rangle\langle -N|_p + |N\rangle\langle N|_p + (\pm 1)^{N+j} (|N\rangle\langle -N|_p + h.c.) \right], \quad (9)$$

which shows strong coherences in the position basis. This feature is preserved for the case of low θ , as demonstrated in Fig. 2 **(b)**, where the fidelity with the target states $\tau_p^j(N - k)$ is substantially larger than the corresponding one for the unconditional state over the whole range of lattice size that we have considered. The analysis at set size of the position space and changing θ presented above is completed by the complementary study against the size of the walker space showcased in Fig. 3 **(a)-(d)**. Fig. 2 **(b)**, Figs. 3 **(c)-(d)**, and Eqs. (8) and (9), showing that the high level of walker-coin entanglement determines coherent superpositions of localised states — implying that the main features of the \hat{Z}_c -walk are retained also for small deviations of the coin parameter from $\theta = 0$.

B. Robustness to dephasing noise

The striking differences between the probability distribution for small- θ DTQRW and the one associated with a Hadamard walk persist under the influences of relevant forms of noise on the walk itself. In light of the transport-like nature of the DTQRW mechanism, and the core role played by interference in the establishment of this salient feature, it is appropriate to focus on a dephasing-like channel $\Phi_p^t[\hat{\rho}_{pc}(t)]$ affecting the position degree of freedom only and that transforms the state $\hat{\rho}_{pc}(t)$ of the walker at time t into

$$\hat{\rho}_{pc}(t) \rightarrow \Phi_p^t[\hat{\rho}_{pc}(t)] = \beta_t \hat{\rho}_{pc}(t) + (1 - \beta_t) \sum_{k=-N}^N |k\rangle\langle k|_p \otimes \hat{\rho}_c^k(t), \quad (10)$$

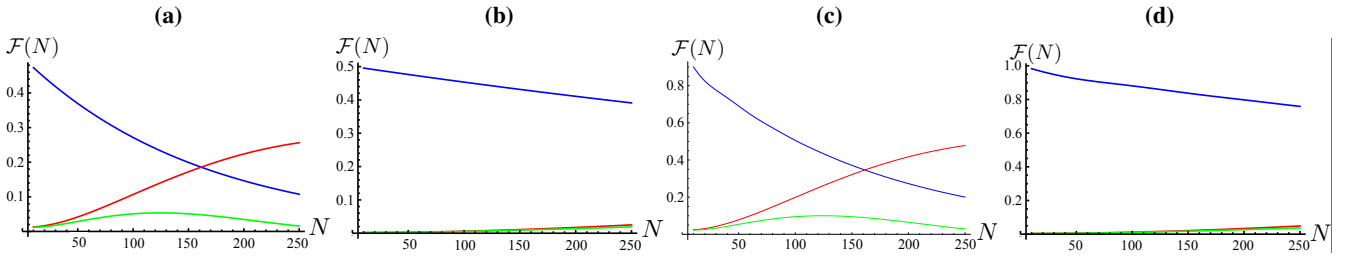


FIG. 3. (Color online) **(a)** State fidelity between the position state of the walker at the end of a $2N + 1$ -site walk (obtained by tracing away the coin's degrees of freedom) with $\theta = \pi/40$ (initial state $|0\rangle_p \otimes |\phi\rangle_c$) and a coherent superposition states of the form $(|-N + k\rangle \pm |N - k\rangle)/\sqrt{2}$. We have considered the cases of $k = 0$ (blue curve), $k = 1$ (red curve), and $k = 2$ (green curve). **(b)** Same as panel **(a)** but for $\theta = \pi/100$. **(c)** and **(d)** Same analysis as in panels **(a)** and **(b)**, respectively, but for a conditional position state achieved by projecting the coin onto $|\phi\rangle_c$ at the end of the walk.

where $\beta_t \in [\delta, 1]$ is a discrete time-dependent noise parameter, whose value we chose randomly at every step of the walk, and $\hat{Q}_c^k(t) = \langle k | \hat{\rho}_{pc}(t) | k \rangle$ are operators in \mathcal{H}_c . Here, $\delta \in [0, 1]$ determines the range of probabilities within which β_t is chosen at a given step of the evolution. In what follows, we will refer to the amplitude $f = 1 - \delta$ of such range as the *noise amplitude*. Therefore, at time t , with probability β_t the mechanism that we consider leaves the state of the walker unaffected, while with a complementary chance it renders it an incoherent admixture of position states, thus erasing any previously set spatial coherence. The dynamics of the walker thus proceeds as follows

$$\hat{\rho}_{pc}(t) = \Phi_p^t [(\hat{S} \hat{C}_c(\theta)) \hat{\rho}_{pc}(t-1) (\hat{S} \hat{C}_c(\theta))^\dagger]. \quad (11)$$

By varying the range within which the values of the set $\{\beta_t\}$ are taken, we go from the ideal case with no noise, to the worst case scenario, the walk in the presence of maximum dephasing effects.

Previous investigations focused on the Hadamard walk have

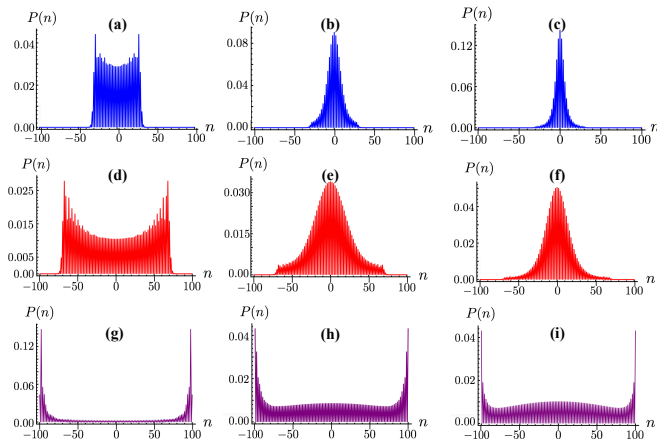


FIG. 4. (Color online) Panels **(a)**-**(c)**: Probability distributions for the DTQRW with initial walker state $|0\rangle_p \otimes |\phi\rangle_c$ for $N = 100$, $\theta = 2\pi/5$ and a growing noise amplitude. We have taken $f = 0.05$ in panel **(a)**, $f = 0.5$ in panel **(b)**, and $f = 1$ in panel **(c)**. Panels **(d)**-**(f)**: Same as above but for $\theta = \pi/4$, thus implementing a Hadamard walk. Panels **(g)**-**(i)**: Same as above but for $\theta = \pi/20$.

shown that, in the presence of maximum noise, the distribution $P(n)$ tends to the Gaussian distribution for a classical walk [14]. On the other hand, small amounts of noise have been shown to be beneficial for the spreading of the walker's distribution, thus demonstrating dephasing assisted-like walk [15]. Here we aim at exploring the resilience of the localization effect observed at small values of θ when the walk is affected as in Eq. (11).

It is instructive to consider first the behaviour of a \hat{Z}_c -walk in the presence of full dephasing noise (*i.e.*, $\theta = \beta_t = 0$). Considering a generic initial pure state for the walker $|\psi_0\rangle_p$, a straightforward calculation shows that after t steps the state of the system is given by

$$\hat{\rho}_{pc}(t) = \frac{1}{2} \left[\hat{\psi}_{-t} \otimes |0\rangle \langle 0|_c + \hat{\psi}_t \otimes |1\rangle \langle 1|_c \right]. \quad (12)$$

In the equation above we have defined the following displaced states of the initial walker state, devoid of all its coherences

$$\hat{\psi}_{\pm t} \equiv \sum_{k=-N}^N |\langle k | \psi_0 \rangle|^2 |k \pm t\rangle \langle k \pm t|_p. \quad (13)$$

Eq. (12) is the incoherent counterpart of Eq. (6) and it shows that, in the presence of full dephasing noise, the system evolves towards an incoherent mixture of the two rigid translations of the walker initial state (devoid of all its coherences). If the initial state is localised in position, we thus have an incoherent mixture of two localised states. Evidently, this is at odds with the behaviour of the Hadamard walk in the presence of full noise, which is instead characterised by a Gaussian like distribution in position. The reason for this discrepancy is that, in the \hat{Z}_c -walk, the coin acts *de facto* as a label that allows to rigidly translate the initial state of the walker towards the opposite ends of the position space, just as we have seen also for the ideal case of Eq. (6). Both cases are then characterized by a localization effect at the extremes of the position space.

Focussing now on the case of intermediate noise and arbitrary coin parameter θ , Fig. 4 summarises the findings of our investigation. For $\theta \geq \pi/4$, increasing noise strengths drive $P(n)$ towards a Gaussian-like distribution that is reminiscent of classical walks. In contrast with this, the localization resulting from the use of small coin parameters survives to arbitrary

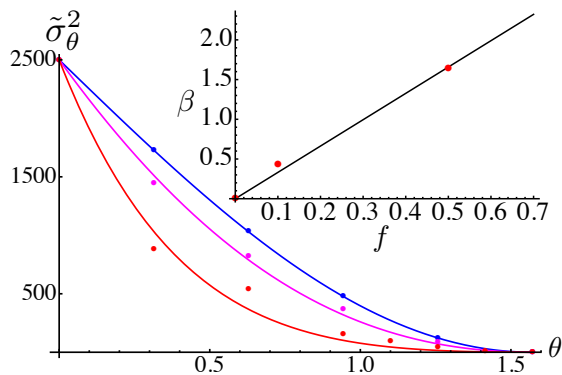


FIG. 5. (Color online) Variance of the probability distribution for the quantum walks with initial walker state $|0\rangle_p \otimes |\phi\rangle_c$ for $N = 50$ against the coin parameter θ for increasing noise strengths. The blue dots are for $\{\beta_t\} = 0$ (blue dots), the magenta ones for $\{\beta_t\} \in [0.9, 1]$, and the red ones for $\{\beta_t\} \in [0.5, 1]$. The solid lines are fits of the form $N^2(1 - \sin \theta)e^{-\beta\theta}$ with β a noise-dependent decay rate. The inset shows the behavior of such parameter against the noise amplitude f .

dephasing strengths, albeit enhancing the probability to find the walker at positions far from the end-lattice ones with respect to the \hat{Z}_c -walk (Fig. 4 only shows a specific instance that does not affect the generality of our conclusions). Such robustness is well illustrated by a study of the variance of the walk distribution: Fig. 5 shows that small values of θ are associated with a variance that remains only mildly affected by growing noise strengths. Differently, for larger values of the coin parameter, even a modest dephasing noise is sufficient to quench the variance of the position distribution, thus favouring the localisation of the particles at the centre of the lattice, a process that occurs, regardless of the strength of noise, at $\theta = \pi/2$ [cf. Fig. 4]. In particular, we have found that the variance of the distribution of the walk at a given amplitude of the range within which $\{\beta_t\}$ is chosen is well described by a modification of the relation in Eq. (4) given by

$$\tilde{\sigma}_\theta^2 = \sigma_\theta^2 e^{-\beta\theta} \sim N^2(1 - \sin \theta)e^{-\beta\theta} \quad (14)$$

with β a noise-dependent effective decay rate that scales linearly with the noise amplitude f [cf. Fig. 5].

III. QUENCHED SPREADING OF DTQRW WITH A SMALL COIN PARAMETER

The localisation features discussed in the previous Sections can be used for the sake of preparing interesting position states of the walker, or to preserve them from the natural dispersion entailed by the walk. Specifically, we first show that the small-coin parameter walk is able to *filter* high-quality coherent superposition states from specific initial position states of the walker.

We start assessing the performance of a walker prepared in superpositions of spatial states. In this section we will see the quantum random walk whose initial position state is a superposition over the Gaussian and uniform distributions. For the

Gaussian distribution, the initial position state is

$$|G\rangle_p = \mathcal{N}_G \sum_n e^{-\frac{n^2}{4\Sigma^2}} |n\rangle_p, \quad (15)$$

where \mathcal{N} is the normalisation constant and Σ is the standard deviation of the Gaussian. Fig. 6 (a) shows the probability distributions for $\Sigma = 10$ and $\theta = \pi/20$, which is chosen here for convenience and clarity of presentation of the results.

Quite clearly, two Gaussian peak appear, both of standard deviation Σ , separated roughly by N . These features should be taken as canonical and valid for other choices of the coin parameter and lattice size. As for the case of a walker starting from the origin of the lattice, though, the distribution $P(n)$ thus found is actually associated with a state that is virtually deprived of coherences. A close inspection of the density matrix of the position degree of freedom only, in fact, reveals the virtual absence of off-diagonal elements. As done in the case of a walk starting from the origin of the lattice, we can enhance the quantum coherence in the position state of the system by projecting the coin onto $|\phi\rangle_c$. This delivers a state that is very close to the quantum coherent superposition of spatial Gaussian distributions as

$$|T\rangle_p = \frac{1}{\sqrt{2}} \sum_n \left[\mathcal{N}_+ e^{-\frac{(n-N/2)^2}{4\Sigma^2}} + \mathcal{N}_- e^{-\frac{(n+N/2)^2}{4\Sigma^2}} \right] |n\rangle_p. \quad (16)$$

Using again state fidelity as a figure of merit for the closeness of the walker's position state to $|T\rangle_p$, we find the results reported in Fig. 6 (b), which demonstrate the very high quality of the conditional state within quite a large range of lattice sizes. Fidelity remains above 92% for $N \simeq 80$, a result that appears to be only very weakly affected by an increase in the variance of the initial Gaussian distribution.

On the other hand, the addition of dephasing noise strongly affects the features of the conditional position states. Already for $\{\beta_t\} \in [0.9, 1]$, the fidelity between the noiseless conditional state and the corresponding noise-affected one drops to $\simeq 0.22$.

IV. EXPERIMENTAL PROPOSAL

Here we present a brief description of a set up that can be used to implement a quantum walk scheme able to generate the sort of coherent state superpositions addressed in our analysis so far. In Fig. 7 (a) we show the optical spatial representation for a 1D DTQRW. In this implementation, the coin is embedded into the walker's degree of freedom, which is embodied by the position of a light pulse, going through a multi-layer interferometer, on a detection line. The walker performs the first step by impinging on a beam splitter with a set reflectivity θ . This effectively implements the coin-tossing operation, and prepares the coin state. The light beam is thus split into a superposition of directions, conditionally on such a coin operation.

In order to reproduce the DTQRW evolution with initial state $\hat{\rho}_{pc}(0)$ in Eq. (5), we propose the following approach: a first coin operation is implemented to generate the state $|\phi\rangle_c$.

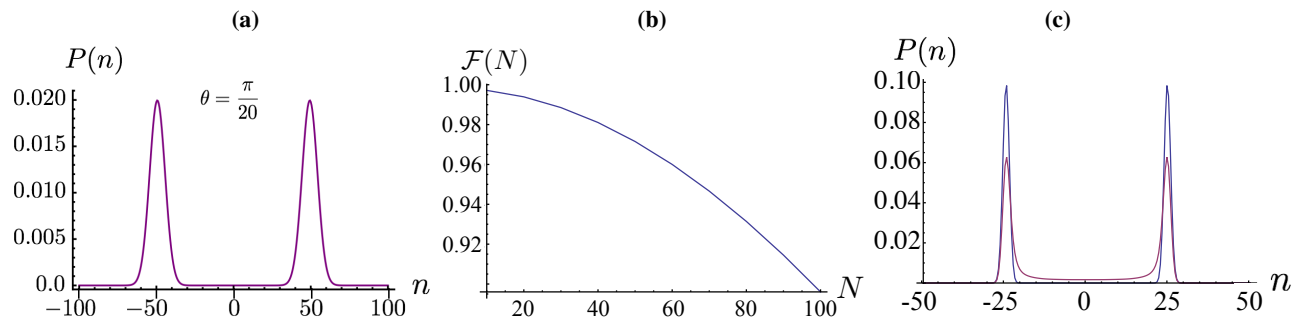


FIG. 6. (Color online) **(a)** Probability distributions $P(n)$ against the site label n for a DTQW with $N = 50$ and the walker prepared in the initial state $|G\rangle_p \otimes |\phi\rangle_c$ with $\Sigma = 10$. **(b)** State fidelity between a Gaussian coherent quantum superposition state of the form in Eq. (16) and the conditional state of the position degree of freedom of a walker initially prepared in Eq. (15) with $\Sigma = 2$ and a growing size N of the lattice. **(c)** Comparison between the spatial probability distributions for a quantum walk with $\theta = \pi/20$ in the absence of noise (blue line) and one achieved by taking $\{\beta_i\} \in [0.9, 1]$ (magenta line). The fidelity between the corresponding states is as low as 0.22.

This can be done through a 50 : 50 beam splitter (i.e. we set the reflectivity ratio $\theta = \pi/4$). The outputs are then re-combined to enter the first beam splitter of the walk [step 0 in Fig. 7 **(b)**]. This is followed by the DTQRW optical scheme, as in Fig. 7 **(a)**, where the beam splitters implementing the necessary series of coin tossing operations have a set reflectivity ratio of $\theta \ll 1$. The process continues up to step N [cf. Fig. 7 **(b)**]. In order to project on the initial coin state, after the final step, we project over the initial coin state inserting another row of beam splitters with $\theta = \pi/4$ and detecting on the output corresponding to $\frac{1}{\sqrt{2}}(|0\rangle + i|1\rangle)$.

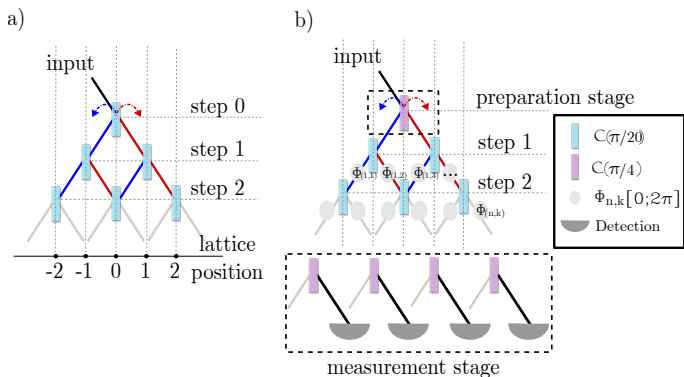


FIG. 7. (Color online) **(a)** Beams propagating through a regular grid of beam splitters achieve a walk with spatial encoding. The powers of beams emerging from a grid of depth N correspond to the probability distribution of the walker and coin (encoded in beam location and direction, respectively) after a walk of N steps. **(b)** Optical scheme for the generation of robust coherent superpositions of position states of the walker. The scheme consists of the preparation of the initial coin state $|\phi\rangle_c = \frac{1}{\sqrt{2}}(|0\rangle + i|1\rangle)$ through a beam splitter at $\theta = \pi/4$ where the output arms are then recombined to allow the walker to start the walk from position 0. The evolution is then performed with a biased coin, beam splitters with transmission ratio θ , and a detection stage. The latter projects the coin onto a desired state through an array of beam splitters at $\theta = \pi/4$ and collecting the output from one side of arms. The phases $\phi_{n,k}$ where n is the step and k the sub-step index, indicate how noise can be inserted in the system.

In this context, an experimental test of the resilience of the localisation phenomenon highlighted in this work can be performed by simulating dephasing noise on the position degree of freedom of the walk, which can be effectively implemented by inserting random phases $\phi_{n,k}$ between the beam splitters of consecutive walk steps. Here n is the step index and k the index of the modes into which the walker is split at a given step of the walk. The strength of such noise will be related to the rate with which we pick each phase between values $(0; 2\pi]$ instead of choosing 0.

A possible platform of the implementation of this scheme is provided by integrated optical waveguide technology [3], where beam splitting operations are realised by optically *writing* on a chip a set of mode couplers, whose mixing ratio (equivalent to our coin parameter), can be chosen during the writing process. Encoding of the walker could be done exploiting the temporal degree of freedom and the coin using polarisation or path degrees of freedom of optical signals. The conditional shift of the walker over the position space can be mapped into earlier and later arrival time given by two different path lengths [9, 17]. This approach would also be suitable for a dynamically variable phase to simulate noise in the system. In order to project over the initial coin state either the last coin operation can be dynamically tuned back to $\theta = \pi/4$ via an electro-optical modulator (EOM) or the outputs can interfere over a beam splitter with $\theta = \pi/4$. The output will consist of a sequence of pulses in time-bins given by the size of the loops; the detection can be achieved through a single-photon avalanche diode with a time-to-digital converter that records the detection time relative to the initial pulse generation. The low losses in such a fibre implementation would allow for the preparation of a superposition state of the form at the core of our study after 20-30 steps evolution.

V. CONCLUSIONS

We have highlighted a phenomenon of coherent localisation of the position of a quantum walker in its position space taking place when the parameter of the coin operation is cho-

sen to be small. Such effect, which is a consequence of the enhanced variance of the quantum walk distribution resulting from the use of a small coin parameter [12] turns out to be a remarkably efficient way to postselect important types of non-classical states. Our scheme offers features of robustness against the range of choices of the coin parameters, and the dephasing noise that might affect the position degree of freedom, while being suitable for agile experimental implementations in state-of-the-art linear optics experiments. Our study paves the way to the investigation of quantum state engineering based on the exploitation of the statistics of quantum walk processes, and reinforces the versatility of such mechanisms for low-control coherent operations on systems spanning naturally large Hilbert spaces.

Note added – While completing this work, we became aware of the work by W.-W. Zhang, *et al.*, *Creating cat states in one-*

dimensional quantum walks using delocalised initial states, arXiv:1605.07539, where the absence of dispersion for delocalised initial states is used to engineer coherent superpositions of position states.

ACKNOWLEDGMENTS

We acknowledge support from the EU project TherMiQ, the Marie Curie ITN PICQUE, the John Templeton Foundation (grant number 43467), the Julian Schwinger Foundation (grant number JSF-14-7-0000), the UK EPSRC (grants EP/M003019/1, and EP/N508664/1), and the Northern Ireland DEL.

-
- [1] J. Kempe, *Contemporary Physics*, **44**, 0303081 (2003).
- [2] H. Jeong, M. Paternostro, and M. S. Kim, *Phys. Rev. A* **69**, 0305008 (2004).
- [3] P. Anderson, *Phys. Rev.* **109**, 1492 (1958); A. Crespi, R. Osellame, R. Ramponi, V. Giovannetti, R. Fazio, L. Sansoni, F. De Nicola, F. Sciarrino, and P. Mataloni, *Nat. Photon.* **7**, 322 (2013).
- [4] S. E. Venegas-Andraca and S. Bose, arXiv:0901.3946 (2009); S. K. Goya and C. M. Chandrashekar, *J. Phys. A* **43**, 235303 (2010); I. Carneiro, *et al.*, *New J. Phys.* **7**, 156 (2005); G. Abal, *et al.*, *Phys. Rev. A* **73**, 042302 (2006); M. Annabestani, M. R. Abolhasani, and G. Abal, *J. Phys. A* **43**, 075301 (2010); C. Di Franco, M. McGettrick, and Th. Busch, *Phys. Rev. Lett.* **106**, 080502 (2011); C. Di Franco, M. McGettrick, T. Machida, and Th. Busch, *J. Comput. Theor. Nanosci.* **10**, 1613 (2013).
- [5] A. Childs, *Phys. Rev. Lett.* **102**, 180501 (2009); A. Childs, D. Gosset, and Z. Webb, *Science* **339**, 791 (2013).
- [6] P. M. Preiss, R. Ma, M. E. Tai, A. Lukin, M. Rispoli, P. Zupancic, Y. Lahini, R. Islam, and M. Greiner, *Science* **347**, 1229 (2015); T. Fukuhara, P. Schauß, M. Endres, S. Hild, M. Cheneau, I. Bloch, and C. Gross, *Nature* **502**, 76 (2013); M. Karski, L. Förster, J.-M. Choi, A. Steffen, W. Alt, D. Meschede, and A. Widera, *Science* **325**, 174 (2009); H. Schmitz, R. Matjeschk, C. Schneider, J. Glueckert, M. Enderlein, T. Huber, and T. Schaetz, *Phys. Rev. Lett.* **103**, 090504 (2009); P. Xue, B. C. Sanders, and D. Leibfried, *Phys. Rev. Lett.* **103**, 183602 (2009).
- [7] F. Zähringer, G. Kirchmair, R. Gerritsma, E. Solano, R. Blatt, and C. Roos, *Phys. Rev. Lett.* **104**, 100503 (2010); D. Bouwmeester, I. Marzoli, G. P. Karman, W. Schleich, and J. P. Woerdman, *Phys. Rev. A* **61**, 013410 (1999); F. Cardano, F. Massa, H. Qassim, E. Karimi, S. Slussarenko, D. Paparo, C. de Lisio, F. Sciarrino, E. Santamato, R. W. Boyd, *et al.*, *Sci. Adv.* **1**, e1500087 (2015); H. B. Perets, Y. Lahini, F. Pozzi, M. Sorel, R. Morandotti, and Y. Silberberg, *Phys. Rev. Lett.* **100**, 170506 (2008); T. Nitsche, F. Elster, J. Novotný, A. Gábris, I. Jex, S. Barkhofen, and C. Silberhorn, arXiv:1601.08204 (2016).
- [8] A. Peruzzo, M. Lobino, J. C. Matthews, N. Matsuda, A. Politi, K. Poulios, X.-Q. Zhou, Y. Lahini, N. Ismail, K. Wörhoff, *et al.*, *Science* **329**, 1500 (2010); L. Sansoni, F. Sciarrino, G. Vallone, P. Mataloni, A. Crespi, R. Ramponi, and R. Osellame, *Phys. Rev. Lett.* **108**, 010502 (2012); A. Regensburger, C. Bersch, B. Hinrichs, G. Onishchukov, A. Schreiber, C. Silberhorn, and U. Peschel, *Phys. Rev. Lett.* **107**, 233902 (2011)
- [9] A. Schreiber, K. N. Cassemiro, V. Potoček, A. Gbris, P. J. Mosley, E. Andersson, I. Jex, and C. Silberhorn, *Phys. Rev. Lett.* **104**, 050502 (2010); A. Schreiber, K. Cassemiro, V. Potoček, A. Gábris, I. Jex, and C. Silberhorn, *Phys. Rev. Lett.* **106**, 180403 (2011).
- [10] S. E. Venegas-Andraca, *Quant. Inf. Process.* **11**, 1015 (2012).
- [11] A. M. Childs, R. Cleve, E. Deotto, E. Farhi, S. Gutmann, and D. A. Spielman, *Exponential algorithmic speedup by a quantum random walk*, In STOC, ACM, 59-68 (2003).
- [12] C. M. Chandrashekar, R. Srikanth, and R. Laflamme, *Phys. Rev. A* **77**, 032326 (2008).
- [13] M.A Nielsen and I.L. Chuang, *Quantum computation and quantum information* (Cambridge University Press, 2010).
- [14] C.M. Chandrashekar, R.Srikanth, and S.Banerjee, *Phys Rev. A* **76**, 022316 (2007).
- [15] V. Kendon and B. Tregenna, *Phys. Rev. A* **67**, 042315 (2003).
- [16] B. Tregenna, W. Flanagan, R. Maile, and V. Kendon, *New J. Phys.* **5**, (2003).
- [17] J. Boutari, A. Feizpour, S. Barz, C. Di Franco, M. S. Kim, W. S. Kolthammer, and I. A. Walmsley, arXiv:1607.00891 (2016).